

## Research Paper

## Night-time light ion transition height behaviour over the Kharkiv (50°N, 36°E) IS radar during the equinoxes of 2006–2010



Dmytro V. Kotov<sup>a,\*</sup>, Vladimír Truhlík<sup>b</sup>, Phil G. Richards<sup>c</sup>, Stanimir Stankov<sup>d</sup>,  
Oleksandr V. Bogomaz<sup>a</sup>, Leonid F. Chernogor<sup>a</sup>, Igor F. Domnin<sup>a</sup>

<sup>a</sup> Institute of Ionosphere, Kharkiv, Ukraine

<sup>b</sup> Institute of Atmospheric Physics, Academy of Sciences of the Czech Republic, Prague, Czech Republic

<sup>c</sup> George Mason University, School of Physics Astronomy and Computational Science, 4400 University Drive, Fairfax, VA, USA

<sup>d</sup> Royal Meteorological Institute, Belgium

## ARTICLE INFO

## Article history:

Received 22 January 2015

Received in revised form

4 June 2015

Accepted 5 June 2015

Available online 10 June 2015

## Keywords:

Ionosphere

Light ions

Transition height

Solar minimum

FLIP

IRI

## ABSTRACT

This research investigates anomalous nighttime ion density behaviour over the Kharkiv, Ukraine incoherent scatter radar (49.6° N, 36.3° E, 45.3° inv) during the equinoxes of 2006–2010. The observations show that the altitude of the transition from O<sup>+</sup> to lighter ions was much lower than empirical and physical models predict. The standard physical model produces very good agreement for the O<sup>+</sup> densities but underestimates the H<sup>+</sup> densities by a factor of 2 in March 2006 and a factor of 3 in March 2009. The anomalously low transition height is a result of similar lowering of the ionospheric peak height and also of significantly increased H<sup>+</sup> density. The lower ionospheric peak height may be caused by weaker nighttime neutral winds. The calculations indicate that the higher measured topside ionosphere H<sup>+</sup> densities are most likely due to higher neutral hydrogen densities. Both factors could be the result of weaker than usual magnetic activity, which would reduce the energy input to high latitudes. Prolonged low activity periods could cause a global redistribution of hydrogen and also allow more neutral hydrogen to settle down from the exosphere into the mid-latitude ionosphere. The finding of the need for higher H densities agrees well with recent H-alpha airglow measurements and it is important for accurate modelling of plasmasphere refilling rates and night-time  $N_mF_2$  values.

© 2015 Elsevier Ltd. All rights reserved.

## 1. Introduction

The ion composition of the ionosphere, topside ionosphere, and plasmasphere has been studied for decades (e.g., Johnson, 1966; Taylor, 1973; Köhnlein, 1981; Heelis et al., 1981; González et al., 1992; Craven et al., 1995; Truhlík et al., 2005; Borgohain and Bhuyan, 2010; Gladyshev et al., 2012; and many others). Most of the important processes are now well understood and the dominant variation patterns have been reproduced by theoretical models and are included in recent empirical models like the International Reference Ionosphere (IRI) (Bilitza et al., 2014). However, the variation of the ion composition with solar activity exhibits some peculiarities which are not accurately reproduced by empirical models. One of the most important parameters

characterizing ion composition is the altitude where the ion gas consists of 50% O<sup>+</sup> and 50% light ions (mostly H<sup>+</sup>, some He<sup>+</sup>). This altitude is called the upper transition height or light ion transition height (H<sub>T</sub>). It depends strongly on latitude and local time and may be used as an anchor point for empirical models of the ionospheric ion composition profile (Bilitza, 1991). Several studies in the past investigated the behaviour of H<sub>T</sub>, mostly dealing with data from low and medium solar activity (e.g., Goel et al., 1976; Titheridge, 1976; Miyazaki, 1979) or with the low altitude OGO-6 data from the solar cycle 20 maximum, which yielded only the night H<sub>T</sub> (Kutiev et al., 1980). Trísková et al. (2001) used ion mass spectrometer data to study H<sub>T</sub> at low and high solar activity up to 2500 km and found a dramatic change of H<sub>T</sub> from solar minima to solar maxima.

There have been few theoretical model-data comparisons of H<sub>T</sub> (MacPherson et al., 1998; Richards et al., 2000; Nanan et al., 2012) because few models are capable of modelling the ionosphere with sufficient precision to compare measured and modelled transition heights. This is because the absolute electron density and its altitude distribution are heavily influenced by neutral winds at mid-latitudes (MacPherson et al., 1998). Unfortunately, neutral winds

\* Corresponding author.

E-mail addresses: [dmitrykotoff@gmail.com](mailto:dmitrykotoff@gmail.com) (D.V. Kotov),  
[vtr@ufa.cas.cz](mailto:vtr@ufa.cas.cz) (V. Truhlík), [prichar1@gmu.edu](mailto:prichar1@gmu.edu) (P.G. Richards),  
[sstankov@meteo.be](mailto:sstankov@meteo.be) (S. Stankov), [albom85@yandex.ru](mailto:albom85@yandex.ru) (O.V. Bogomaz),  
[Leonid.F.Chernogor@univer.kharkov.ua](mailto:Leonid.F.Chernogor@univer.kharkov.ua) (L.F. Chernogor),  
[domninpro@mail.ru](mailto:domninpro@mail.ru) (I.F. Domnin).

are hard to measure and empirical models are too unreliable for detailed model-data comparisons. This wind effect is most clearly manifested in the changes in the height of the peak electron density ( $h_m F_2$ ). The problem of uncertainty in neutral wind can be addressed by adjusting the neutral wind to closely match the observed  $h_m F_2$  as it steps in time, as done, for example, by the field line interhemispheric plasma (FLIP) model (Richards, 1991). Richards et al. (2000) modelled the  $H^+/O^+$  ratio at 500 km for January 6–12, 1997 at Millstone Hill and found good agreement, although there was a lot of scatter in the data.

During the last solar minimum, extremely low solar activity in 2008–2009 led to significant changes in the geospace environment. For instance, the thermospheric density and temperature were at record low values during this period (Solomon et al., 2010). The topside ionosphere was also significantly contracted, as demonstrated by anomalous  $H_T$  values observed by in situ measurements and incoherent scatter radar (Heelis et al., 2009; Klenzing et al., 2011; Aponte et al., 2013). Using C/NOFS satellite data, Klenzing et al. (2011) found that  $H_T$  moved down to 475–490 km after midnight. The smallest  $H_T$  values (450–470 km) were recorded over the Arecibo IS radar (Aponte et al., 2013). However, the C/NOFS mission was limited to  $\pm 13^\circ$  latitude. The Arecibo IS radar is located at  $18^\circ$  geographic latitude but, with a magnetic latitude of approximately  $30^\circ$ , it has some characteristics of a mid-latitude station. This is significant because the plasmasphere plays an important role in determining the upper transition height. However, until now there have been no data on the  $H_T$  behaviour at middle latitudes during the 2007–2009 extreme solar minimum.

In this study we present an analysis of the diurnal minimum of the light ion transition height  $H_{T\min}$  using night-time equinox data from the Kharkiv incoherent scatter (IS) radar facility ( $49.6^\circ N$ ,  $36.3^\circ E$ ,  $45.3^\circ$  inv) from 2006 to 2010. The IRI-2012 empirical model and the FLIP physical model are used to interpret some of the surprising features of the data.

## 2. IS facility and data set

The Kharkiv IS radar is located in Ukraine ( $49.6^\circ N$ ,  $36.3^\circ E$ ,  $45.3^\circ$  inv). It operates at 158 MHz and uses a zenith-directed 100-m diameter fixed antenna (Domnin et al., 2013). Measured auto-correlation functions (ACFs) of IS signal (19 lags, sampling rate is  $30.5 \mu s$ ) are used to estimate ionospheric plasma parameters by least squares fitting to the theoretical ACFs. Some features of the fitting technique are distinctive. Details are presented in Appendix A.

In the topside mode, the transmitter is operated using 650- $\mu s$  uncoded pulses with a 40-ms interpulse period giving data on the electron density, ion and electron temperatures, and ion composition with height resolution of 100 km. Our calculations demonstrate that in such a case biases in plasma parameters caused by the range smearing of measured ACFs are considerably smaller than the statistical errors. The main errors in  $H_T$  are statistical errors of the measured fractions of  $H^+$  and  $He^+$  ions (see Appendix A). The  $F_2$ -layer peak height may be overestimated because of height smearing up to 5–10 km at night and up to 15–20 km during the day.

Measured the peak electron density ( $N_m F_2$ ) values from an ionosonde located near the IS radar are used to calibrate the IS electron and ion densities profiles. The upper boundary altitude for the IS measurements depends on heliogeophysical conditions and ranges from 500 to 550 km in winter at solar minimum up to 900 to 1200 km in summer at solar maximum.

The results presented in this paper are obtained with one hour temporal resolution. All the obtained equinox data from 2006 to

2010 were used for the analysis: i.e. March 30, September 21, 2006; March 21, September 27, 2007; March 20, September 24, 2008; March 25, September 30, 2009; March 24, September 21, 2010.

## 3. Models used

### 3.1. IRI-2012

The International Reference Ionosphere (IRI) is an empirical standard model of the ionosphere based on a large database of monthly medians of electron density, ion composition, electron temperature, and ion temperature in the altitude range from 50 km to 2000 km (Bilitza et al., 2014). This paper used the Ne-Quick-option (Radice, 2009), which is the recommended option for calculating the electron density in the topside ionosphere. The standard settings were used for calculating the  $N_m F_2$  and the  $h_m F_2$  values. The IRI ion composition was obtained from the model developed by Trísková et al. (2003), which is the recommended option since the deployment of IRI-2007 (TTS-03). This newer model takes advantage of better global coverage provided by satellite ion mass spectrometer measurements (Interkosmos-24, AE-C, AE-E) and uses the invariant dip latitude coordinate that is close to the magnetic inclination (dip) near the magnetic equator and closer to invariant latitude at higher latitudes and thus correlates well with the observed variation patterns of the topside ion distribution (Truhlík et al., 2001).

### 3.2. FLIP model

The Field Line Interhemispheric Plasma (FLIP) model is a one-dimensional model that calculates the plasma densities and temperatures along entire magnetic flux tubes from below 100 km in the Northern hemisphere through the plasmasphere to below 100 km in the Southern hemisphere (Richards, 2001; Richards et al., 2010a). The Earth's magnetic field is represented by a dipole that has a tilt that is adjusted as a function of longitude so as to produce a close representation of the actual field in the ionosphere.

The equations solved are the continuity and momentum equations for  $O^+$ ,  $H^+$ ,  $He^+$ , and  $N^+$ . The energy equations are solved for ion and electron temperatures. The equations are solved using a flux-preserving formulation together with a Newton iterative procedure that has been described by Torr et al. (1990). Electron heating due to photoelectrons is provided by a solution of the two-stream photoelectron flux equations using the method of Nagy and Banks (1970). The photoelectron solutions have been extended to encompass the entire field line on the same spatial grid as the ion continuity and momentum equations. Chemical equilibrium densities are obtained for  $NO^+$ ,  $O_2^+$ ,  $N_2^+$ ,  $O^+(^2P)$ , and  $O^+(^2D)$  ions below 500 km altitude in each hemisphere. The densities of minor neutral species  $NO$ ,  $O(^1D)$ ,  $N(^2D)$ , and  $N(^4S)$  are obtained by solving continuity and momentum equations from  $\sim 100$  to  $\sim 500$  km in each hemisphere. The model also solves for the first five excited states of vibrationally excited  $N_2$ . Significant amounts of vibrationally excited  $N_2$  can enhance the loss of  $O^+$  by increasing the  $O^+ + N_2$  reaction rate.

The solar EUV fluxes are important because they are not only responsible for ion production but also for the photoelectrons that heat the thermal electrons. The calculations in this paper use an accurate model of the solar EUV irradiances based on measurements by the SEE instrument on the TIMED satellite (Woods et al., 2008). The SEE solar EUV fluxes have been shown to produce very good agreement between measured and modelled  $N_m F_2$  during the 2006–2009 solar minimum period (Richards et al., 2009, 2010b,

2014). The primary heat source for thermal electrons is the photoelectron flux, which is calculated by the FLIP model from the solar EUV fluxes (Richards et al., 2006). There is an additional source of electron heat from electron quenching of  $N(^2D)$  (Richards, 1986). The FLIP model ion-neutral cooling rates were taken from Schunk and Nagy (1978). The 3 main cooling processes of thermal electrons are (1) Coulomb collisions with ions, (2) fine structure excitation of atomic oxygen, and (3) vibrational excitation of  $N_2$ . There is cooling by vibrational excitation of  $O_2$  as well as rotational excitation of  $O_2$  and  $N_2$  and excitation of  $O(^1D)$  but these are minor above 250 km. The FLIP model electron-ion cooling rate was taken from Itikawa (1975). The model chemical reaction rates have been updated (Richards, 2011) to those published by Fox and Sung (2001). For the neutral atmosphere, the FLIP model uses the revised MSIS model, NRL Mass Spectrometer, Incoherent Scatter Radar Extended model (NRLMSISE-00) (Picone et al., 2002). The NRLMSISE-00 model  $O_2$  densities are not much different at solar minimum but they are a factor of 2 smaller at solar maximum than in previous MSIS models (Hedin, 1987).

The degree of electron heating in the plasmasphere is a significant uncertainty for topside modelling. The heating may come from photoelectron trapping or ring current particles. This uncertainty was overcome for the calculations in this paper, by constraining the FLIP model to follow the measured topside electron temperature using the algorithm developed by Richards et al. (2000). This algorithm continually adjusts the plasmaspheric heating rate as the model steps in time to closely follow the topside temperature, while still calculating the temperature at all altitudes in the usual way.

## 4. Results

### 4.1. Dependence on solar activity

Fig. 1 shows changes in the observed  $H_{Tmin}$  values, which usually occurs between 00:00 and 04:00 LT. Between March 30, 2006 and September, 2007  $H_{Tmin}$  decreased by 78 km and then increased by 83 km between September 2009 and September

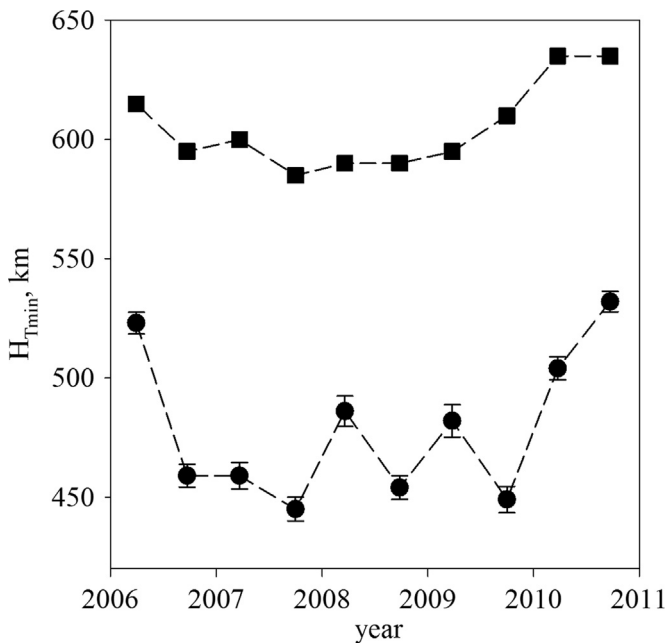


Fig. 1. Changes in upper transition height observed over Kharkiv IS radar for equinoxes between 2006 and 2010 (circles) and corresponding IRI-2012 model calculations (squares).

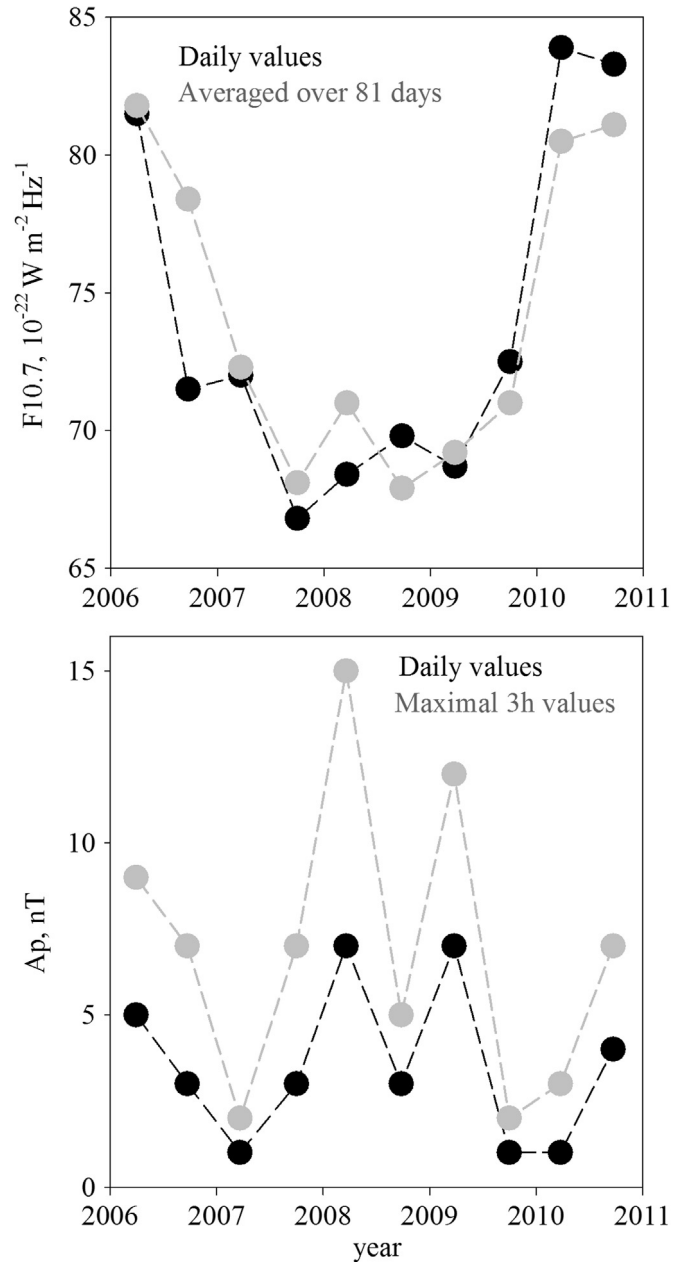


Fig. 2. F10.7 indices (top panel) and Ap indices (bottom panel) for the days preceding the dates under study.

2010. These relative changes are comparable to the relative changes in F10.7 index ( $\approx 17\%$ ) (Fig. 2, Table 1). The  $H_{Tmin}$  variations are well correlated with changes in the daily F10.7 index ( $F10.7_D$ ) and its 81 day average ( $F10.7_{81}$ ): the linear correlation coefficient  $r(H_{Tmin}, F10.7_D) \approx 0.81$ , and  $r(H_{Tmin}, F10.7_{81}) \approx 0.77$ . The errors at the 0.95 confidence probability are  $\epsilon_{0.95} \approx 0.40$  and 0.50 respectively. The rate  $\Delta H_{Tmin}/\Delta F10.7_D$  is about 6 km per solar flux unit.

Few studies have dealt with the solar activity dependence of  $H_{Tmin}$ . Trísková et al. (2003) and Truhlík et al. (2005) found substantial changes in  $H_T$  with increasing solar activity at equatorial and mid-latitudes for daytime and nighttime. For nighttime at mid-latitudes in the interval of F10.7 from 80 to 115  $H_T$  increased by about 2.9 km per solar flux unit (Truhlík et al., 2005) that is a factor of 2 less than the Kharkiv ISR observations. For the period we consider, Aponte et al. (2013) showed (using Arecibo ISR data) nighttime increase of  $H_T$  by about 4.6 km per solar flux unit which

**Table 1**  
3-h Ap indices (numbers on the right is UT, LT for Kharkiv is  $\approx$  UT+2.4) and solar activity indices (daily F10.7<sub>D</sub> and its 81 day average F10.7<sub>81</sub>) for the day of the IS measurements and the previous day.

Year	Month	Day	Ap00	Ap03	Ap06	Ap09	Ap12	Ap15	Ap18	Ap21	F10.7 <sub>D</sub>	F10.7 <sub>81</sub>
2006	March	29	4	7	3	4	3	3	6	9	82	82
2006	March	30	5	3	2	2	2	2	6	7	84	82
2006	September	21	0	2	3	4	4	3	3	3	72	78
2006	September	22	0	2	0	2	2	2	4	2	73	78
2007	March	20	0	0	0	0	2	2	2	2	72	73
2007	March	21	0	0	3	2	3	2	0	0	72	73
2007	September	26	7	5	3	4	2	0	4	2	67	68
2007	September	27	3	0	0	12	6	48	39	32	67	68
2008	March	19	0	4	6	4	12	15	9	9	68	72
2008	March	20	6	6	4	7	18	12	7	7	68	72
2008	September	23	5	0	4	3	3	2	2	2	70	68
2008	September	24	2	3	2	5	4	2	0	0	69	68
2009	March	24	3	12	7	7	12	7	5	6	69	70
2009	March	25	18	22	7	7	3	3	4	6	68	70
2009	September	29	2	0	2	2	2	2	0	0	73	71
2009	September	30	6	5	5	3	6	3	6	5	72	71
2010	March	23	2	0	0	0	3	2	2	0	83	81
2010	March	24	0	0	0	2	7	9	3	5	84	81
2010	September	20	3	6	2	3	3	3	7	2	83	81
2010	September	21	6	12	7	4	2	0	0	3	85	80

is consistent with our observations.

#### 4.2. The surprising latitudinal inversion of $H_{Tmin}$

Solar activity related changes in the neutral atmosphere cannot explain the unusually small  $H_{Tmin}$  values for the seemingly ordinary solar activity conditions of March 30, 2006 and March 24 and September 21, 2010. The daily F10.7 indices on these days were close to the average equinoctial values in 1974, which is the year of the AE-C mission ion composition data that were primarily used for the IRI model ion densities. However, the  $H_{Tmin}$  values observed at Kharkiv are 100 km less than the IRI values (Fig. 1). Moreover, the recently observed latitudinal variations of  $H_{Tmin}$  have the opposite behaviour to that predicted by earlier in situ measurements and the IRI-2012 model. For seemingly typical solar minimum conditions in 2006 and 2010, the  $H_{Tmin}$  over Kharkiv was up to 50 km lower than over the equator (Klenzing et al., 2011) and up to 10 km lower than over Arecibo (Aponte et al., 2013) (Fig. 3).

Given the different  $H_{Tmin}$  values for similar solar activity conditions, this paper addresses the hypothesis that the unusual  $H_T$  behaviour is related to the low magnetic activity during the 2006–2010 period.

#### 4.3. $H_T$ dependence on magnetic activity

It is difficult to separate solar and geomagnetic activity effects on the ionosphere and no systematic study has considered the impact of geomagnetic activity on  $H_T$ . This is especially true for studies involving in-situ data, which require considerable averaging to obtain  $H_T$  (Trísková et al., 2001). Trísková et al. (1998) showed a substantial upward movement of the transition surface during a geomagnetic storm. The current IRI model does not produce changes in  $H_T$  caused by geomagnetic activity.

Fig. 2 and Table 1 show the behaviour of the Ap index for the days before the dates under consideration. Based on available IS data, it can be shown that the approximate dependence of  $H_{Tmin}$  on solar and magnetic activity is  $H_{Tmin} = 4.3F10.7 + 4Ap + 135$  for the range of F10.7<sub>D</sub> values (67–84) under consideration here. It indicates that the sensitivity of  $H_{Tmin}$  to Ap changes can be linearly represented as  $\Delta H_{Tmin}/\Delta Ap \approx 4$  km/nT. Therefore, it is likely that the observed increase in  $H_{Tmin}$  for spring 2008, 2009 was caused by a moderate increase in magnetic activity.

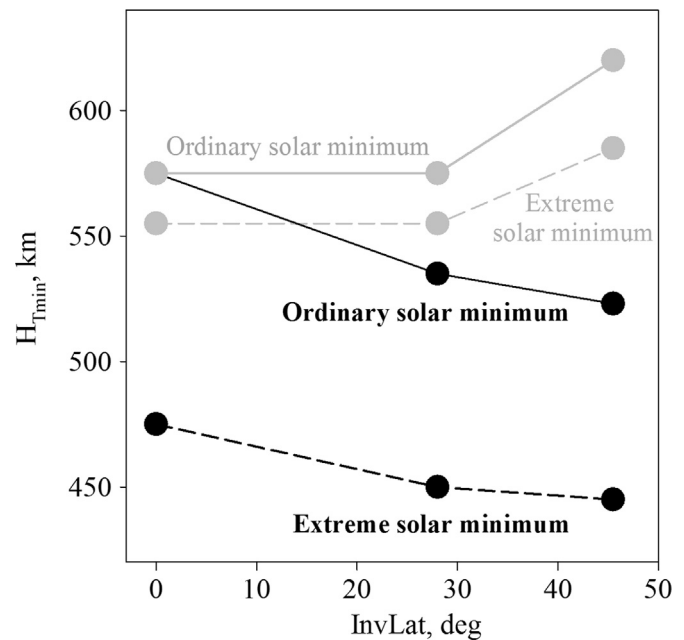


**Fig. 3.** Latitudinal variations in  $H_{Tmin}$ . Black lines show recent equinoctial C/NOFS, Arecibo and Kharkiv IS radars data, grey lines – earlier in situ data (IRI model).

Fig. 4 shows that the average Ap index for the periods around the equinoxes in 1974 was 10–25 nT more than the average Ap values for March 30, 2006 and March 24 and September 21, 2010. The different Ap values could explain the observed  $H_{Tmin}$  differences of  $\approx 100$  km between IRI and IS data.

The significant  $H_T$  dependence on Ap values can also explain the relatively small  $\Delta H_{Tmin}/\Delta F10.7_D$  value in IRI since the satellite data selection criteria included geomagnetic activity up to  $K_p=4$  ( $Ap=27$ ). The Kharkiv data show that even weak geomagnetic disturbances can increase  $H_T$  considerably.

#### 4.4. Correlation with $h_mF_2$ variations. $H_{Tmin}/h_mF_2$ ratio

The height of the peak electron density ( $h_mF_2$ ) is estimated from the IS electron density profiles concurrently with  $H_{Tmin}$ . Fig. 5 shows that the observed  $h_mF_2$  decreases by about 37 km from

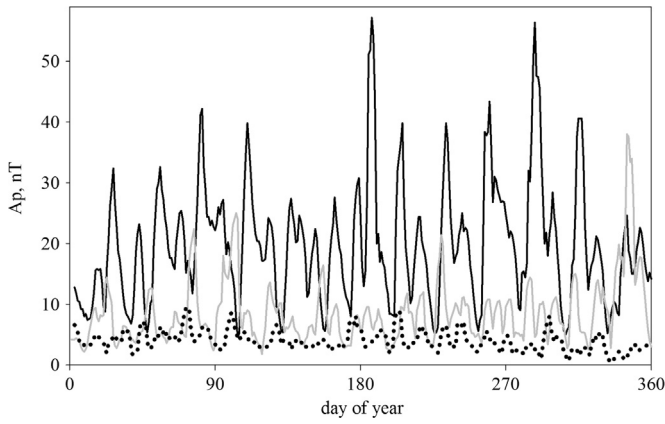


Fig. 4. Ap indices averaged within 5 days. Solid black line corresponds to 1974, solid grey line – 2006, points – 2009.

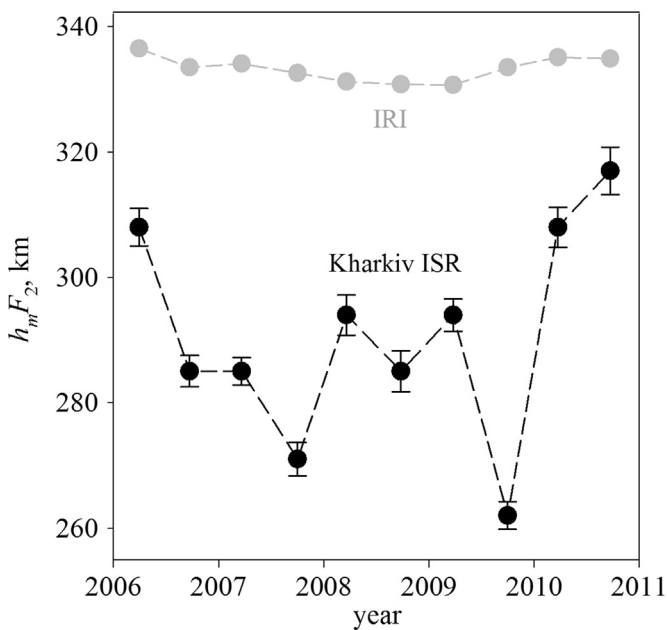


Fig. 5. Changes of F2-layer peak height over Kharkiv IS radar at points in time when  $H_{Tmin}$  were registered and corresponding IRI-2012 values.

March 2006 to September 2007 and increases by about 64 km from September 2009 to September 2010. The corresponding changes in  $h_mF_2$  from the IRI-2012 model are less than 4 km. The linear correlation coefficients from the data are  $r(h_mF_2, F10.7_D) \approx 0.76$  ( $\epsilon_{0.95} \approx 0.50$ ). It is seen from the IS results that and  $\Delta h_mF_2 / \Delta Ap \approx (3.0 \pm 1.5) \text{ km/nT}$ .

The observed  $h_mF_2$  in Fig. 5 and the  $H_{Tmin}$  in Fig. 1 are closely related with a correlation coefficient  $r(h_mF_2, H_{Tmin}) \approx 0.94$  ( $\epsilon_{0.95} \approx 0.18$ ). The  $h_mF_2$  and  $H_{Tmin}$  coupling is less strong in the IRI model:  $r(h_mF_2, H_{Tmin}) \approx 0.74$  and  $\epsilon_{0.95} \approx 0.50$ . The variability and thickness (F2-layer peak – upper transition height) of the topside region are also significantly greater in the data than in the IRI model. The difference  $H_{Tmin} - h_mF_2$  decreased up to 15% from March 2006 to September 2009, whereas the IRI model gives a negligible decrease. In March 2006, the IRI model gives  $\approx 64$  km higher values for the difference  $H_{Tmin} - h_mF_2$  ( $\approx 30\%$  more than in the IS radar data). In September 2009, the observed topside thickness was up to 90 km ( $\approx 54\%$ ) less than the IRI. These results demonstrate that the topside ionosphere was strongly contracted during the last solar minimum and markedly compressed in comparison with IRI pattern even for ordinary solar minimum conditions.

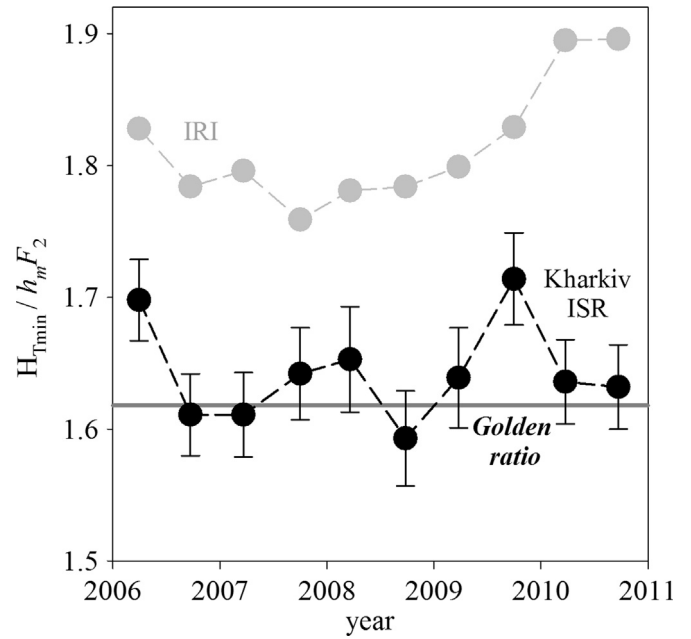


Fig. 6. Changes in  $H_{Tmin}/h_mF_2$  ratio over Kharkiv IS radar.

The main finding is that the observed nighttime  $h_mF_2$  is up to 30 km lower than the IRI values for ordinary solar minimum and up to 70 km lower for 2008–2009. The most likely reason for the relatively low F2-layer peak location is that the nighttime equatorward winds were smaller during the 2006–2010 period due to the lower geomagnetic activity which caused lower energy input to the high latitude region. It is well known that increased magnetic activity can greatly increase mid-latitude nighttime winds (Frey et al., 1996; Ishii et al., 1999).

The strong correlation between  $H_{Tmin}$  and  $h_mF_2$  is not surprising because when the ionosphere is lowered the  $O^+$  density is decreased at all altitudes. This allows the  $H^+$  from the plasmasphere to settle further down into the topside ionosphere. The  $H_{Tmin}$  sensitivity to changes in  $h_mF_2$  is represented by  $\Delta H_{Tmin} / \Delta h_mF_2 \approx (2.2 \pm 1.3)$ .

Fig. 6 compares  $H_{Tmin}/h_mF_2$  from observations with the IRI model. It is interesting that the observed ratio remained relatively unchanged during 2006–2010 in spite of the dramatic changes in other topside parameters (linear correlation coefficient  $r(H_{Tmin}/h_mF_2, F10.7_D) \approx 0.25$ ,  $r(H_{Tmin}/h_mF_2, Ap_{max}) \approx 0.09$ ). We note that the relative variation of the IRI  $\Delta H_{Tmin} / \Delta h_mF_2$  tracks the data reasonably well from 2006 until 2009, but then the IRI values are much higher in 2010. This may indicate that the nighttime ionosphere is recovering more slowly than normal from the deep solar minimum.

It is interesting to note that  $H_{Tmin}/h_mF_2 \approx \phi$ ,  $\phi = 1.618\dots$  is the “golden ratio” (e.g., Livio, 2002) (the average  $H_{Tmin}/h_mF_2 \approx 1.643$ , standard deviation for averaged value is 0.025). This fact demonstrates also that nighttime  $h_mF_2$  and topside thickness were related according to the equation  $h_mF_2 / (H_{Tmin} - h_mF_2) \approx \phi$  under equinoctial solar minimum condition.

#### 4.5. Simulations

In this section the FLIP model is used to explore the hypothesis that the unusually low observed  $H_T$  values could be caused by weak geomagnetic activity.

The FLIP model was run for March 30, 2006 and March 25, 2009 and geographic coordinates of the Kharkiv IS radar. The FLIP model calculates the ion densities along the magnetic field that

passes through  $\sim 250$  km altitude directly over Kharkiv while the measurements are made in the vertical direction. The model densities were not interpolated to the vertical because the geographic latitude along the field line changes by less than  $2^\circ$  between 250 and 600 km altitude.

The most important requirement for accurate modelling of the electron density is to reproduce the observed  $h_m F_2$ , which is primarily dependant on the neutral winds at mid-latitudes. The FLIP model can automatically adjust neutral winds to accurately reproduce the observed  $h_m F_2$  (Richards, 1991). The resultant winds are termed equivalent or effective winds because changes in  $h_m F_2$  may also be caused by zonal electric fields. Nevertheless, several studies have shown good agreement with optical wind measurements (e.g., Dyson et al., 1997; Richards et al., 2009) indicating that the electric field usually plays a minor role at mid-latitudes. The FLIP model was run with a maximum time resolution of 10 min using the actual values of solar and magnetic activity indices.

Table 1 shows the 3 h magnetic activity indices ( $A_p$ ) and the daily and 81-day average F10.7 indices for the days of the measurements and the previous days.

The FLIP model was run for 5 days before the day of the observations to allow the plasmasphere to reach equilibrium, which is appropriate for the weak magnetic conditions. Additionally, the model used the measured  $T_e$  values at the height of 473 km to better match the plasma temperature altitude profiles.

Fig. 7 shows the measured and calculated profiles of the  $O^+$ ,  $H^+$  and  $He^+$  densities for midnight for March 30, 2006. The first calculation was made using the local time variation of the observed  $h_m F_2$  values as a wind proxy (Richards, 1991). This calculation gives good agreement with the measured  $O^+$  profile, underestimating the  $N_m F_2$  by only 20% during the night. However, the measured  $H^+$  densities exceed the model densities by a factor of 1.6 at the height of 550 km and by a factor of 2.6 at 450 km. On the other hand, the model overestimates the  $He^+$  density by a factor

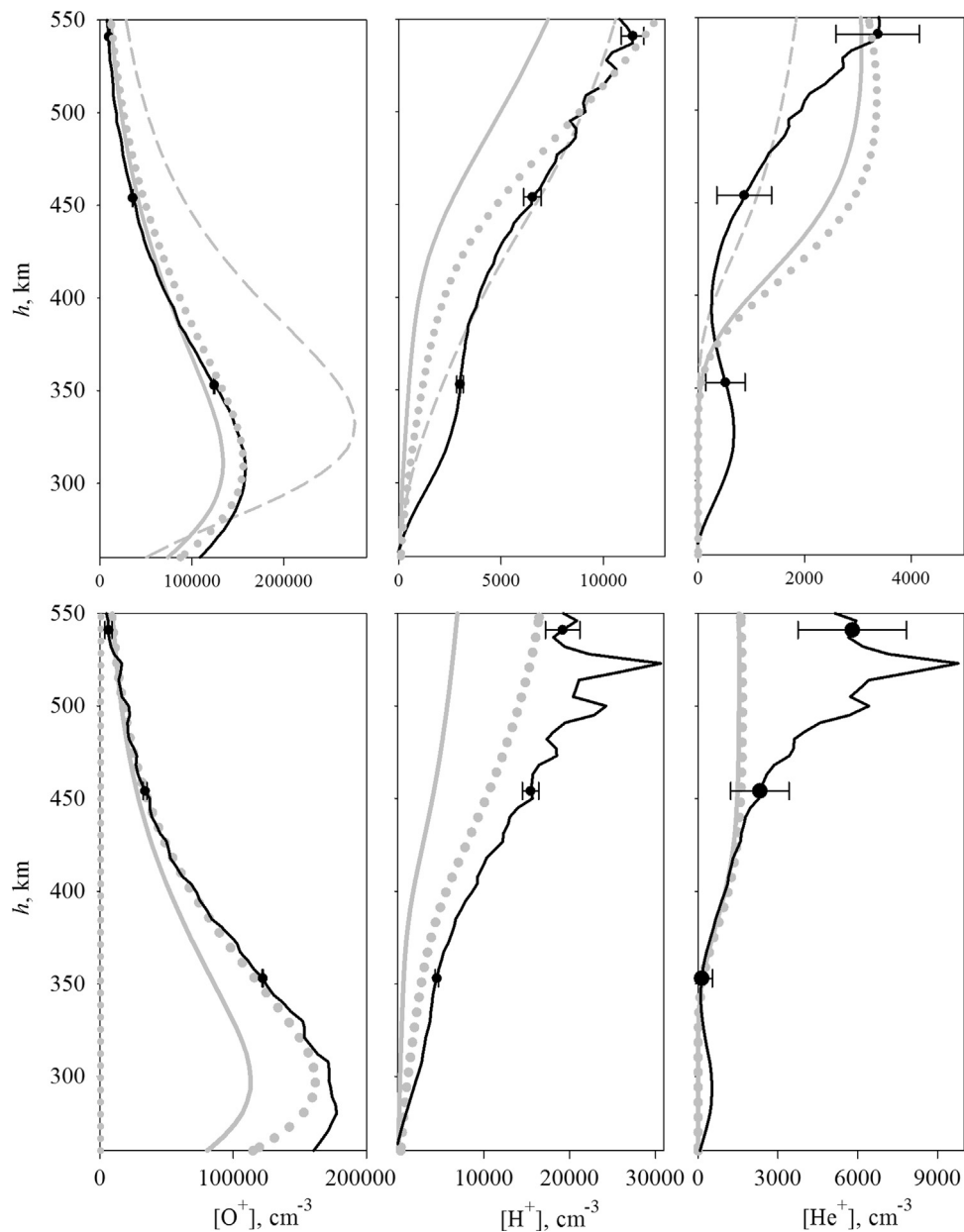
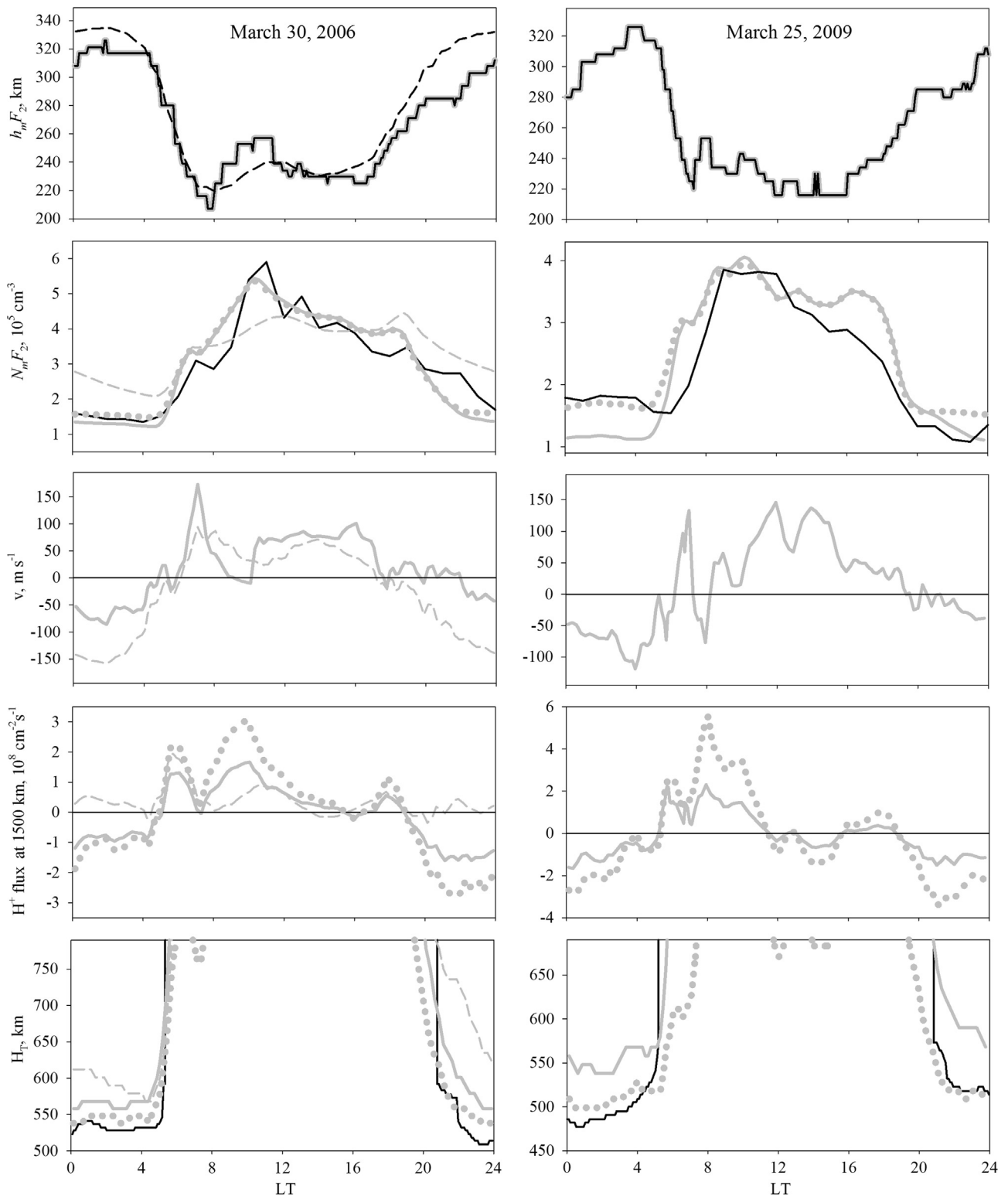


Fig. 7. Height profiles of  $O^+$ ,  $H^+$  and  $He^+$  densities obtained by the Kharkiv IS radar (solid black line) and calculated by FLIP model using Kharkiv IS radar  $h_m F_2$  values (solid grey line) and IRI  $h_m F_2$  values (dashed grey line) for 00:00 LT on March 30, 2006 (top panels) and on March 25, 2009 (bottom panels). Grey dots show the FLIP results when Kharkiv IS radar  $h_m F_2$  values were used and the NRLMSIS model H density was increased by a factor of 2 (for March 30, 2006) and by a factor of 3 (for March 25, 2009).



**Fig. 8.** Diurnal variations of  $h_mF_2$ ,  $N_mF_2$ , horizontal wind velocity  $v$  at  $F_2$ -layer peak height,  $H^+$  flux at 1500 km, and upper transition height. The solid black line shows the Kharkiv IS radar data, the solid grey line shows the model results using the Kharkiv IS radar  $h_mF_2$ , and the dashed grey line shows the model results using the IRI  $h_mF_2$  (shown by black dashed line). Grey dots show the FLIP results when Kharkiv IS radar  $h_mF_2$  values were used and the NRLMSIS model H density was increased by a factor of 2 (for March 30, 2006) and by a factor of 3 (for March 25, 2009).

of 2 near 450 km. More importantly, the shape of the model  $He^+$  profile is very different. If the model reproduced the  $He^+$  density, the model  $H_T$  would be decreased by about 10 km. It should be noted that data analysis allows detection of  $H^+$  and  $He^+$  ions when their fraction is more than 1% of total ion density. This

means, that the estimated  $H^+$  and  $He^+$  ion densities are not reliable when they are less than  $1500\text{ cm}^{-3}$ . At midnight, the FLIP model  $H_T$  is  $\approx 558$  km, which is 35 km greater than the measured value but is 80 km lower than the IRI value (Fig. 8, fifth panel). The behaviour of the diurnal variations of the measured and calculated

$H_T$  is similar.

The second model calculation was made using the IRI  $h_m F_2$  data for March 30, 2006 as a wind proxy. It is seen that there is a very good agreement between the ISR and IRI  $h_m F_2$  data from sunrise to sunset (Fig. 8, first panel). But after midnight and in the evening, the IRI model overestimates  $h_m F_2$  by 20–40 km. The FLIP model calculation shows that such  $h_m F_2$  differences lead to a factor of 2 increase in  $N_m F_2$  by midnight. Fig. 8 (third panel) demonstrates that the nighttime horizontal wind velocity from the IRI  $h_m F_2$  is a factor of 3 higher than that obtained from the measured  $h_m F_2$ . Such results support the hypothesis that nighttime equatorward winds were significantly weakened during the March 30, 2006. The FLIP model midnight  $H_T$  is  $\approx 45$  km higher using the IRI  $h_m F_2$ . The  $H_T$  dependence on neutral wind through  $h_m F_2$  changes could explain the observed latitudinal inversion of  $H_{Tmin}$  (Fig. 3) because the sensitivity of  $h_m F_2$  to equatorward winds decreases from middle to low latitudes due to the decreasing geomagnetic field inclination. It is likely, that during magnetic disturbances, the nighttime wind is stronger leading to higher  $h_m F_2$  (and  $H_T$ ) at mid-latitudes compared to low latitudes. When the wind is weak, the midlatitude  $h_m F_2$  is reduced and  $H_T$  probably can be as low as at low latitudes or even lower.

The model calculated  $\Delta H_T / \Delta h_m F_2 \approx 1.8$  agrees well with the observations. Fig. 7 reveals that the higher  $h_m F_2$  from the IRI model not only raises the whole layer, but also allows  $O^+$  to decay more slowly in the topside leading to a greater change in  $\Delta H_T$  than  $\Delta h_m F_2$ . The increase in  $h_m F_2$  increases the  $H^+$  density by a factor of 1.6 at 550 km but the  $O^+$  density increases by a factor of 3 causing a greater increase in  $H_T$  than in  $h_m F_2$ .

The FLIP model underestimation of the  $H^+$  density even when there is excellent agreement for the topside  $O^+$  density suggests that the problem may lie with the neutral hydrogen density. The fact that the problem also occurs in the chemical equilibrium region below 400 km means that the problem cannot be solved by simply invoking additional plasmaspheric  $H^+$ . It is important to note that the measured ion temperature ( $T_i$ ) was close to the NRLMSIS neutral temperature  $T_n$  at night (Fig. 9) as it is for the

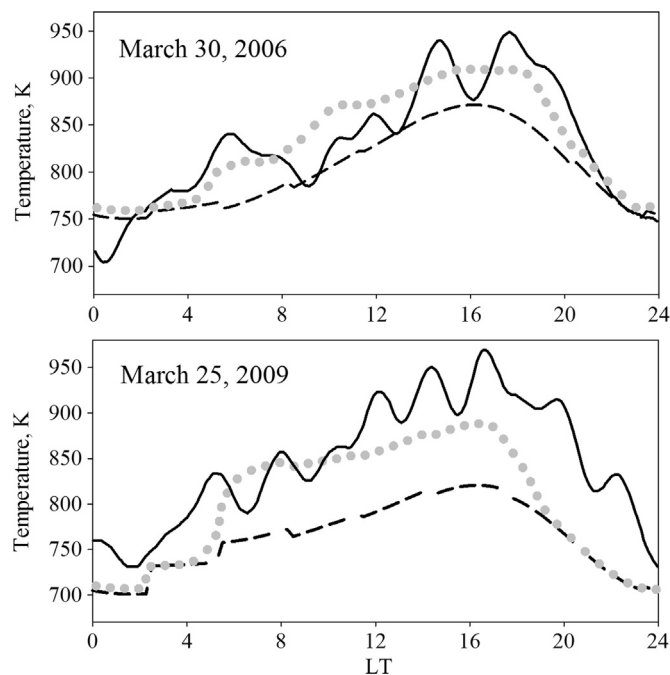


Fig. 9. Diurnal variations of  $T_i$  obtained by the Kharkiv IS radar (solid line),  $T_i$  calculated by the FLIP model using the Kharkiv IS radar  $h_m F_2$  (dots), and corresponding  $T_n$  from NRLMSIS model (dashed line) for March 30, 2006 (top panel) and for March 25, 2009 (bottom panel). All results relate to the height 335 km.

FLIP  $T_i$  values. The daytime  $T_i$  values are about 30–60 K above  $T_n$  and also are close for both FLIP and IS data. The agreement between the measured and modelled temperatures gives confidence in the NRLMSISE-00 model  $O_2$ ,  $N_2$ , and  $O$  densities which are based on large data sets for various conditions. In contrast, the NRLMSISE-00H density is based on a much more limited data set from the AE-C and AE-E satellites, and it was obtained indirectly from the measured  $O$ ,  $O^+$ , and  $H^+$  densities assuming chemical equilibrium (Hedin, 1983).

As noted earlier, the solar activity during the 1974 and 2006 equinoxes was similar but the magnetic activity was markedly stronger in 1974 than in 2006. The NRLMSISE-00 model  $T_n$  was  $\approx 50$ –100 K higher in 1974 than it was in 2006 due to these differences. The extrapolation of the dependence of the NRLMSIS H density on  $T_n$  to the much lower values in 2006–2009 may not be accurate. Prolonged low activity periods could cause a global redistribution of hydrogen and also allow more neutral hydrogen to settle down from the exosphere into the mid-latitude ionosphere.

Additional FLIP model calculations were made to determine the effect of increasing the H density. Figs. 7 and 8 show that doubling the H density increases the modelled  $H^+$  density by a factor of 1.7 at 550 km giving very good agreement with observations. At the height of 450 km, FLIP now underestimates the  $H^+$  density by only 30%. The increased H density increases the  $H^+$  density in the chemical equilibrium region below 450 km as expected, but it also increases the density in the diffusive region by increasing the plasmasphere density. Stronger filling of the plasmasphere during the day leads to enhanced downward  $H^+$  flux in the evening. It is notable that the enhanced plasmaspheric  $H^+$  flux also increases the  $O^+$  density by  $\sim 20\%$  in the vicinity of the F2-layer peak height leading to even better agreement between the modelled and measured  $N_m F_2$  throughout the night. Finally, the modelled midnight  $H_T$  now is almost equal to observed values during the night (within  $\approx 20$  km). Simply doubling the H density at all altitudes is justified because of its very large scale height ( $\sim 1000$  km).

Figs. 7 and 8 also show the same model calculations using the measured peak height as the wind proxy for March 25, 2009. In this case, the H density had to be increased by a factor of 3 to produce satisfactory agreement for the  $H^+$  density. There was no justification for changing the densities of all the other neutral species from the NRLMSIS values because the measured  $T_i$  values were close to the actual NRLMSIS  $T_n$  at night (Fig. 9). As in 2006, it is clearly seen that the increased H density led not only to much better agreement for  $H^+$  profile but also to better agreement for the  $O^+$  density. The FLIP model  $N_m F_2$  increased by a factor of 1.5 with the larger H density. With the improved ion densities, there is also very good agreement with the measured  $H_T$  diurnal variations as the model  $H_T$  is lowered by  $\approx 40$ –75 km.

There is a possible explanation for a greater increase in the NRLMSIS H density on March 25, 2009 than on March 30, 2006 even though the  $T_n$  values are similar for both dates (Fig. 9). That is, there was a prolonged (3 years) period with very quiet geomagnetic activity between March 30, 2006 and March 25, 2009.

In March 2009, the measured  $He^+$  density is about 3 times higher than in 2006 at 450 km and the profile shape is very different. There is excellent model-data agreement below 450 km but the model greatly underestimates the measured  $He^+$  density near 500 km. It would be difficult to explain all the difference as a result of increased  $He^+$  diffusion from the plasmasphere because that would also affect the region below 450 km.

#### 4.6. Comparison of ISR electron density profiles with LIEDR and IRI results

The upper transition height is an important parameter for monitoring the topside ionospheric plasma density distribution.

For example, the development of the operational system for deducing the vertical distribution of the electron density in the local ionosphere (Stankov et al., 2011). The system, dubbed Local Ionospheric Electron Density profile Reconstruction (LIEDR), acquires and processes in real time the concurrent and collocated ionosonde and GNSS measurements, and ultimately, deduces a full-height electron density profile based on a reconstruction technique proposed by Stankov et al. (2003). In this approach, the vertical electron density profile at a given location is deduced from ground-based measurements of the total electron content (TEC), ionospheric vertical soundings, and empirically-obtained values of the  $O^+/H^+$  ion transition height (Stankov, 2002). The retrieval of the corresponding electron density distribution is performed in two main stages: construction of the bottomside electron profile (below  $h_mF_2$ ) and construction of the topside profiles (above  $h_mF_2$ ). High-precision ionosonde measurements are used for directly obtaining the lower part of the electron density profile based on Epstein layer functions utilising measured values of the critical frequencies,  $f_oF_2$  and  $f_oE$ , the peak heights,  $h_mF_2$  and  $h_mE$ , and the propagation factor, M3000F2. The corresponding bottomside part of TEC is calculated from this profile and is then subtracted from

the entire TEC in order to obtain the unknown portion of TEC in the upper part. The topside TEC (TEC<sub>top</sub>) is used in the next stage for deducing the topside ion and electron profiles. In this way, the topside profile is more adequately represented because of the use of additional information about the topside ionosphere, such as the values of TEC and  $O^+/H^+$  ion transition height.

Clearly, the LIEDR system offers opportunities for gaining a deeper understanding of the physical processes, and the drivers behind these processes, in the local ionosphere. However, direct comparisons between LIEDR calculations and ISR radar measurements would be of great benefit for the improvement of the (topside) ion and electron density modelling. To demonstrate this, the LIEDR model was run with data from the ISR measurements carried out at 00:00 LT on March 30, 2006 and on March 25, 2009. The key input parameters ( $N_mF_2$ ,  $h_mF_2$ , and  $H_T$ ) were deduced directly from the measured ISR profiles and the TEC values were taken from the TEC global ionospheric maps provided by the Center for Orbit Determination in Europe (CODE). Four different ionospheric profilers – Exponential, Epstein,  $\alpha$ -Chapman, and  $\beta$ -Chapman were tried in the LIEDR calculations.

The results are presented in Fig. 10. In each panel, the vertical

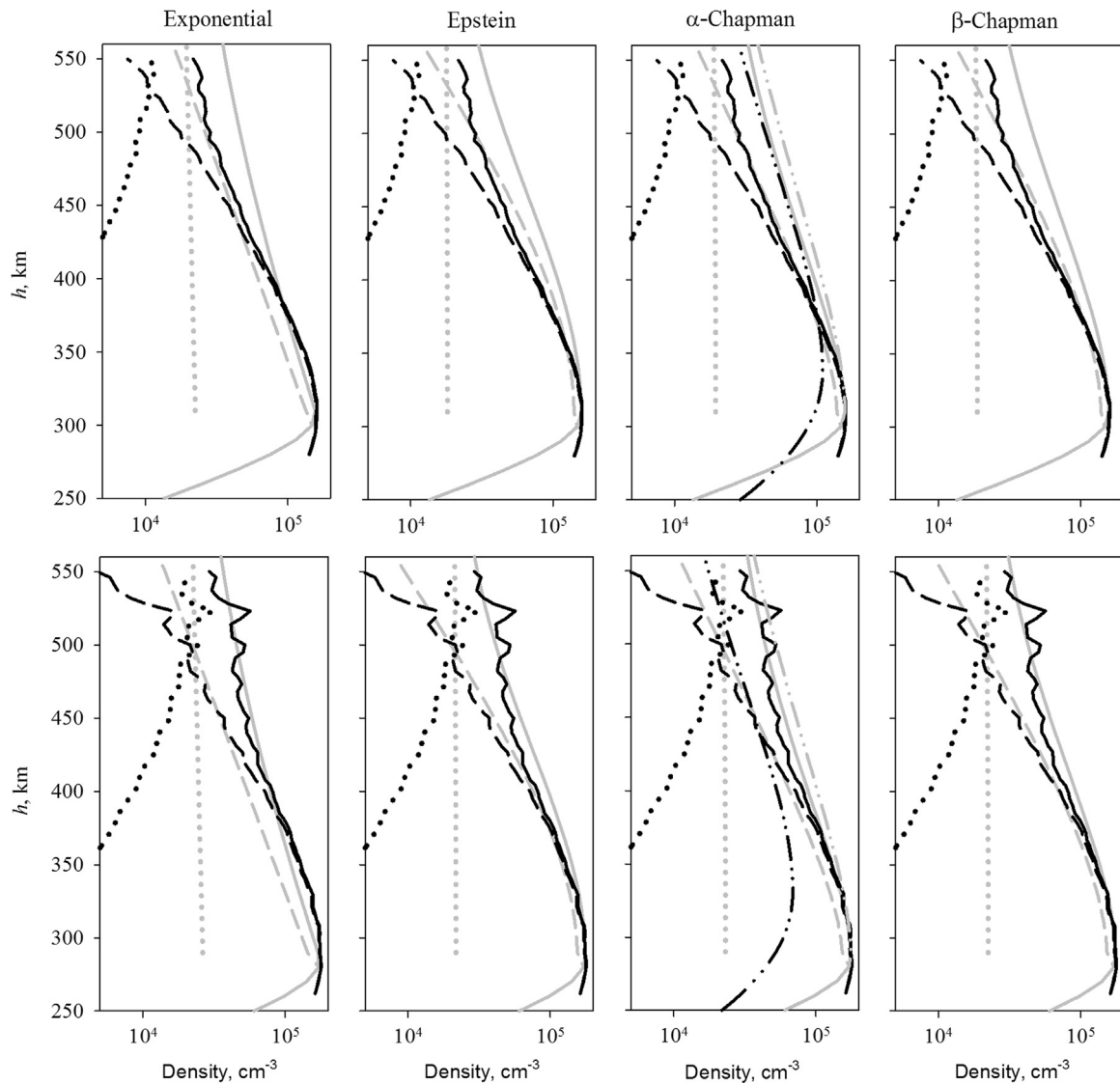


**Fig. 10.** Comparison of ion and electron density profiles as obtained by LIEDR calculations (grey lines) and ISR measurements (black lines) at midnight on March 30, 2006 (top panels) and on March 25, 2009 (bottom panels). Solid lines show electron density, dashed lines –  $O^+$  density, dots –  $H^+$  density. Four different LIEDR profilers have been tried – Exponential, Epstein,  $\alpha$ -Chapman and  $\beta$ -Chapman. Dash-dot lines show electron density calculated by LIEDR using IRI upper transition height (grey) and by NeQuick model (black).

$O^+$ ,  $H^+$ , and electron density profiles, calculated with one of the above mentioned profilers, are plotted together with the profiles obtained from ISR measurements. Overall, the results are good, especially for the lower upper ionosphere, given that some input parameters could not be provided with high accuracy, such as TEC and  $M3000F_2$ . In terms of proximity to the “real” (ISR-measured) profiles, it appears that, in these two particular cases, the Chapman profilers yield better results, followed by the Epstein profiler. The Exponential profiles are too “sharp” at the peak height and as a result, the ion (electron) density is substantially underestimated just above the peak and well overestimated at higher altitudes. The  $H^+$  density profile is obviously not adequately calculated below the  $O^+/H^+$  transition height, and this issue needs to be addressed. The modelling of the ion and electron density profiles is better in the case of the March 25, 2009. The discrepancies observed between the modelled and measured profiles on March 30, 2006 are most probably due to an inaccurate TEC value which was taken from a global map due to lack of GNSS measurements at the site. Also, since ionosonde measurements were not available too, an inaccurate  $M3000F_2$  value could be the reason for the sharper decrease of the modelled electron density below the peak height. However, the availability of accurate measurements of the  $O^+/H^+$  transition height was very important – the IRI transition height used in LIEDR would offer about 25% larger values than the measured, which leads to a similar overestimation of the LIEDR topside electron density.

Comparison of the observed electron density profiles with IRI calculations shows a need for improvement for both  $F_2$ -layer peak and topside regions (Fig. 10). The IRI model underestimates  $N_mF_2$  by a factor of 1.45 for March 30, 2006 and by a factor of 2.55 for March 25, 2009. At the height of 500 km, IRI overestimates electron density by 45% for March 30, 2006 and underestimates it by 85% for March 25, 2009. Such differences can be explained taking into account the fact that IRI model gives averaged electron density profiles obtained under various geomagnetic conditions including disturbed ones when the neutral temperature was higher and, as a result, nighttime neutral wind was enhanced,  $F_2$ -layer was shifted upward, and H density was decreased leading to weakening of nighttime downward plasmasphere  $H^+$  fluxes.

## 5. Discussion and conclusions

The Kharkiv IS radar (49.6° N, 36.3° E, 45.3° inv) observational results reveal that the light ion transition height  $H_T$  was anomalously low for the solar activity conditions during the period of 2006–2010. The diurnal minimum of  $H_T$  was 100–150 km lower than the IRI-2012 prediction, which is well outside the estimated standard deviation of the  $H_T$  measurements (see Appendix A). The anomalously low  $H_T$  values occurred between 22:00 LT to 05:00 LT (see Fig. 8) for each of ten dates considered. Taking into account the 1 h time resolution for our data, this means that there are about 80 independent  $H_T$  estimates for the period of 2006–2010.

We attribute the low  $H_T$  location to the unprecedented low magnetic activity. There are three possible explanations for why lower magnetic activity would decrease the transition height at mid-latitudes, (1) the lower neutral temperature would decrease the topside O density and increase the topside H density, (2) lower magnetic activity may reduce the nighttime equatorward wind thereby lowering the  $F_2$ -peak height and the upper transition height, and (3) the contraction of the thermosphere would produce a lower  $h_mF_2$  just as happens between solar maximum and solar minimum. The IRI-2012 model, which includes geomagnetic activity variations, does not show significant magnetic activity related changes in  $h_mF_2$  during this period.

The FLIP model was able to reproduce the observed  $O^+$  density

profile when  $h_mF_2$  was constrained by the measured values. The calculations show that the difference between the observed and IRI  $h_mF_2$  could result from a factor of 3 decrease in the nighttime equatorward neutral wind velocity, which would correspond to a similar lowering of the upper transition height. On the other hand the model underestimated the observed  $H^+$  density by factors of 2–3 even at altitudes that should be in chemical equilibrium. Given the good agreement between the observed and modelled  $O^+$  density, the most likely explanation is that the NRLMSISE-00 model H density is too low by a similar factor. The increased H density directly increases the  $H^+$  density in the chemical equilibrium region below ~450 km and also in the diffusive region due to enhanced downward nighttime  $H^+$  fluxes to the ionosphere. There is some support for higher H densities from Nossal et al. (2012) who found that the H densities from the NRLMSISE-00 model underestimate the measured H-Alpha airglow intensities by a factor of 2.

These results have important implications for the rate of plasmasphere refilling, which is most closely tied to the H density in the topside ionosphere and less so to the topside plasma temperatures (Richards and Torr, 1985). Under equilibrium conditions, the flow of  $H^+$  into the plasmasphere is limited because it has to diffuse through  $O^+$  before it can escape. Models indicate that this happens at an altitude where the  $O^+$  density decreases to about  $5 \times 10^4 \text{ cm}^{-3}$ . Only  $H^+$  produced above this altitude can escape. Thus, other factors such as winds and changes in the major neutral species, that can affect the  $O^+$  density, have little effect on the  $H^+$  outflow. Recently Denton and Borovsky (2012) have determined that some models severely underestimate the refilling rate at geosynchronous orbit ( $L=6.6$ ) after a magnetic storm in June 2007. Our calculations with the FLIP model (not shown) indicate that the plasmasphere refilling rate is increased by more than a factor of 2 when the NRLMSISE-00H density is increased by a factor of 3 but no other changes are made to the model inputs. These refilling rates agree well with those observed by Denton and Borovsky (2012). Other calculations have found that the refilling rate varies significantly with longitude. Simulations in the American sector would underestimate the maximum refilling rate observed at geosynchronous orbit by more than 50%.

The model-data  $He^+$  density differences are difficult to explain because there is no significant local nighttime source of  $He^+$  and it is not in chemical equilibrium above 300 km. Therefore, the topside  $He^+$  comes from the plasmasphere. Reactions with  $N_2$  are the main sink for  $He^+$ . The nighttime measurements resemble a daytime profile that would occur when  $He^+$  is diffusing into the plasmasphere.

The results could also explain the unexpectedly high nighttime critical frequencies of  $F_2$ -layer ( $foF_2$ ) at mid-latitudes during the period of 2007–2009 (Zakharenkova et al., 2011). According to data obtained by ionosonde in Juliusruh (54.6 N, 13.4 E), midnight equinoctial  $foF_2$  values were 20–25% higher than IRI-2007 predictions (Zakharenkova et al., 2011), i.e.  $N_mF_2$  values were about 50% more than expected. Such a pattern agrees well with our observations (compare the ISR and IRI-2012 electron density profiles in Fig. 10) and can be obtained by simulation only when we use a factor of 3 higher neutral hydrogen densities (Figs. 7 and 8). Thus, this effect could be named the thermosphere hydrogen anomaly.

## Acknowledgements

D. Kotov is grateful to Joseph D. Huba (Naval Research Laboratory, Plasma Physics Division, United States, Washington, D.C.) for helpful discussions. V. Truhlik was supported by grant

1507281J of the Grant Agency of the Czech Republic. S. Stankov acknowledges the support by the Royal Meteorological Institute (RMI) via the Belgian Solar-Terrestrial Centre of Excellence (STCE).

## Appendix A

We did the following simulations to demonstrate the fact that biases in electron and ion densities and in plasma temperatures caused by height smearing of measured ACFs are insignificant when we use 650  $\mu$ s pulse.

A. We simulated the ‘measured’ ACF  $R^*(\tau, h)$  using a forward model  $R^*(\tau, h) = \int_{-\infty}^{\infty} \int_0^{\infty} d\theta dr R_{IS}(\theta, r) W_{\tau}(\theta, r)$ , where  $W_{\tau}(\theta, r) = \int_{-\infty}^{\infty} \int_{-\infty}^{\infty} ds dr W_{\tau}(s, r) W_{\tau+\tau}(s + \theta, r)$  is a two-dimensional radar ambiguity function,  $W_{\tau}(s, r) = g(t - s)p\left(s - \frac{2r}{c}\right)$ ,  $g(t)$  is impulse response function of the receiver,  $p(t)$  is the transmitted pulse shape which defines the range extent of the scattering volume,  $t = \frac{2h}{c}$ ,  $R_{IS}(\theta, r)$  is ACF of IS signal scattered at the height  $r$  (e.g., Holt et al., 1992; Hysell et al., 2008).

We used the actual parameters from the radar topside mode ( $g(t)$  and  $p(t)$  functions) to calculate  $W_{\tau}(\theta, r)$  function. Height profiles of electron density, plasma temperatures and different ion fractions for various heliogeophysical conditions, seasons, and local times from IRI-2012 model were used to calculate different possible height distributions of  $R_{IS}(\theta, r)$  functions. Additionally we used triangular summation rule for ‘measured’ ACFs (Holt et al., 1992) to get the same height resolution for all ACF lags (100 km) as we do in reality with our data.

B. We solved inverse problem for  $R^*(\tau, h)$  functions to obtain ‘measured’ plasma parameters. We did this as in reality, using for least squares fitting the triangular sum of functions  $R_M(\tau, h) = \int_{-\infty}^{\infty} \int_0^{\infty} d\theta dr R^*(\theta, r) \rho(\theta) W_{\tau}(\theta, r)$ , where  $\rho(\theta)$  is theoretical ACF of IS signal for a given plasma parameters which are assumed to be unchanged within the height. This approach is intermediate between gated analysis (e.g., Hysell et al., 2009) and full-profile analysis (e.g., Holt et al., 1992; Hysell et al., 2008) because of we use the forward model to calculate the lag product matrices (e.g., Hysell et al., 2009) which are then compared with measurements but assume that only IS signal power changes with height.

Our simulations showed that involving of even smoothed ‘measured’ IS power profile  $R^*(0, h)$  into calculation markedly reduces biases in estimates of plasma temperatures and ion fractions. Biases in  $T_i$  and  $T_e$  do not exceed several tens of Kelvins at  $F_2$ -layer peak and in the topside (biases reach 150–200 K when IS signal power height changes are ignored). Bias of electron density in the topside is no more than 15% at night and does not exceed 25% during the day.

Absolute biases of  $H^+$  and  $He^+$  fractions do not exceed 2% (biases up to 10% occur when IS signal power height changes are ignored) that is notably less comparing with statistical errors (near  $H_T$ , bias of  $H^+$  fraction is usually close to zero). Thus we can conclude that only statistical errors of  $H^+$  and  $He^+$  fractions affects the accuracy of  $H_T$  estimates. This accuracy depends on standard deviation of total  $H^+ + He^+$  fraction  $\sigma_F$  at the height where this total fraction is equal 50% (for one hour time averaging, from the data set  $\sigma_F \approx 5$ –7%) and on height gradient at this height  $\frac{\Delta \text{Fraction}(H^+ + He^+)}{\Delta h}$  ( $\approx 0.7\%/km$  for conditions under consideration). Because the  $H^+ + He^+$  fraction changes almost linearly in a wide region of values around the value 50% (as follows from the data set), the standard deviation of  $H_T$  can be linearly represented as  $\sigma(H_T) \approx \sigma_F \left[ \frac{\Delta \text{Fraction}(H^+ + He^+)}{\Delta h} \right]^{-1}$ . In our case  $\sigma(H_T) \approx 7$ –10 km.

## References

- Aponte, N., Brum, C.G.M., Sulzer, M.P., Gonzales, S.A., 2013. Measurements of the  $O^+$  to  $H^+$  transition height and ion temperatures in the lower topside ionosphere over Arecibo for equinox conditions during the 2008–2009 extreme solar minimum. *J. Geophys. Res. Space Phys.* 118, 4465–4470. <http://dx.doi.org/10.1002/jgra.50416>.
- Bilitza, D., 1991. The use of transition heights for the representation of ion composition. *Adv. Space Res.* 11 (10), 183–186.
- Bilitza, D., Altadill, D., Zhang, Y., Mertens, C., Truhlik, V., Richards, P., McKinnell, L.-A., Reinisch, B., 2014. The International Reference Ionosphere 2012 – a model of international collaboration. *J. Space Weather Space Clim.* 4, A07.
- Borghain, A., Bhuyan, P.K., 2010. Solar cycle variation of ion densities measured by SROSS C2 and FORMOSAT-1 over Indian low and equatorial latitudes. *J. Geophys. Res.: Space Phys.* 115 (A4), A04309.
- Craven, P.D., Comfort, R.H., Richards, P.G., Grebowsky, J.M., 1995. Comparisons of modeled  $N^+$ ,  $O^+$ ,  $H^+$ , and  $He^+$  in the midlatitude ionosphere with mean densities and temperatures from Atmosphere Explorer. *J. Geophys. Res.: Space Phys.* 100 (A1), 257–268.
- Denton, M.H., Borovsky, J.E., 2012. Magnetosphere response to high-speed solar wind streams: a comparison of weak and strong driving and the importance of extended periods of fast solar wind. *J. Geophys. Res.: Space Phys.* 117 (A9), A09L05.
- Domnin, I.F., Yemel'yanov, L. Ya, Kotov, D.V., Lyashenko, M.V., Chernogor, L.F., 2013. Solar Eclipse of August 1, 2008, above Kharkov: 1. Results of incoherent scatter observations. *Geomagn. Aeron.* 53 (1), 113–123.
- Dyson, P.L., Davies, T.P., Parkinson, M.L., Reeves, A.J., Richards, P.G., Fairchild, C.E., 1997. Thermospheric neutral winds at southern mid-latitudes: a comparison of optical and ionosonde hmF2 methods. *J. Geophys. Res.: Space Phys.* 102 (A12), 27189–27196.
- Fox, J.L., Sung, K.Y., 2001. Solar activity variations of the Venus thermosphere/ionosphere. *J. Geophys. Res.: Space Phys.* 106 (A10), 21305–21335.
- Frey, H.U., Haerendel, G., Knudsen, D., Buchert, S., Bauer, O.H., 1996. Optical and radar observations of the motion of auroral arcs. *J. Atmos. Terr. Phys.* 58, 57–69.
- Gladyshev, V.A., Shchekotov, A.Y., Yagova, N.V., Berthelie, J.J., Parrot, M., Akent'eva, O.S., Baranskii, L.N., Fedorov, E.N., Mulyarchik, T.M., Molchanov, O.A., 2012. Concentration of ions in the topside ionosphere as measured onboard the DEMETER satellite: morphology and dependence on solar and geomagnetic activity. *Cosm. Res.* 50 (2), 103–115.
- Goel, M.K., Rao, B.C.N., Chandra, S., Maier, E.J., 1976. Satellite measurements of ion composition and temperatures in the topside ionosphere during medium solar activity. *J. Atmos. Terr. Phys.* 38 (4), 389–394.
- González, S.A., Fejer, B.G., Heelis, R.A., Hanson, W.B., 1992. Ion composition of the topside equatorial ionosphere during solar minimum. *J. Geophys. Res.: Space Phys.* 97 (A4), 4299–4303.
- Hedin, A.E., 1983. A revised thermospheric model based on mass spectrometer and incoherent scatter data: MSIS-83. *J. Geophys. Res.: Space Phys.* 88 (A12), 10170–10188.
- Hedin, A.E., 1987. MSIS-86 thermospheric model. *J. Geophys. Res.: Space Phys.* 92 (A5), 4649–4662.
- Heelis, R.A., Murphy, J.A., Hanson, W.B., 1981. A feature of the behavior of  $He^+$  in the nightside high-latitude ionosphere during equinox. *J. Geophys. Res.: Space Phys.* 86 (A1), 59–64.
- Heelis, R.A., Coley, W.R., Burrell, A.G., Hairston, M.R., Earle, G.D., Perdue, M.D., Power, R.A., Harmon, L.L., Holt, B.J., Lippincott, C.R., 2009. Behavior of the  $O^+$  /  $H^+$  transition height during the extreme solar minimum of 2008. *Geophys. Res. Lett.* 36, L00C03. <http://dx.doi.org/10.1029/2009GL038652>.
- Holt, J.M., Rhoda, D.A., Tetenbaum, D., van Eyken, A.P., 1992. Optimal analysis of incoherent scatter radar data. *Radio Sci.* 27 (N3), 435–447.
- Hysell, D.L., Rodrigues, F.S., Chau, J.L., Huba, J.D., 2008. Full profile incoherent scatter analysis at Jicamarca. *Ann. Geophys.* 26, 59–75.
- Hysell, D.L., Chau, J.L., Huba, J.D., 2009. Topside measurements at Jicamarca during solar minimum. *Ann. Geophys.* 27, 427–439.
- Ishii, M., Oyama, S., Nozawa, S., Fujii, R., Sagawa, E., Watari, S., Shinagawa, H., 1999. Dynamics of neutral wind in the polar region observed with two Fabry–Perot interferometers. *Earth Planet. Space* 51, 833–844.
- Itikawa, Y., 1975. Electron-ion energy transfer rate. *J. Atmos. Terr. Phys.* 37 (12), 1601–1602.
- Johnson, C.Y., 1966. Ionospheric composition and density from 90 to 1200 km at solar minimum. *J. Geophys. Res.* 71 (1), 330–332.
- Klenzing, J., Simões, F., Ivanov, S., Heelis, R.A., Bilitza, D., Pfaff, R., Rowland, D., 2011. Topside equatorial ionospheric density and composition during and after extreme solar minimum. *J. Geophys. Res.* 116, A12330. <http://dx.doi.org/10.1029/2011JA017213>.
- Köhnlein, W., 1981. On the diurnal and seasonal variations of  $H^+$ ,  $He^+$ ,  $N^+$ ,  $O^+$ , and  $Ne$  at 1400-km altitude. *Planet. Space Sci.* 29 (7), 775–782.
- Kutiev, I., Heelis, R.A., Sanatani, S., 1980. The behavior of the  $O^+$ – $H^+$  transition level at solar maximum. *J. Geophys. Res.: Space Phys.* 85 (A5), 2366–2372.
- Livio, M., 2002. *The Golden Ratio: The Story of Phi, The World's Most Astonishing Number*. Broadway Books, New York.
- MacPherson, B., González, S.A., Bailey, G.J., Moffett, R.J., Sulzer, M.P., 1998. The effects of meridional neutral winds on the  $O^+$ – $H^+$  transition altitude over Arecibo. *J. Geophys. Res.* 103, 29183–29198. <http://dx.doi.org/10.1029/98JA02660>.
- Miyazaki, S., 1979. Ion transition height distribution obtained with the Satellite

- Taiyo, J. Geomagn. Geoelectr. 31, S113–S124.
- Nagy, A.F., Banks, P.M., 1970. Photoelectron fluxes in the ionosphere. *J. Geophys. Res.* 75 (31), 6260–6270.
- Nanan, B., Chen, C.Y., Rajesh, P.K., Liu, J.Y., Bailey, G.J., 2012. Modeling and observations of the low latitude ionosphere–plasmasphere system at long deep solar minimum. *J. Geophys. Res.* 117, A08316. <http://dx.doi.org/10.1029/2012JA017846>.
- Nossal, S.M., Mierkiewicz, E.J., Roesler, F.L., 2012. Observed and modeled solar cycle variation in geocoronal hydrogen using NRLMSISE-00 thermosphere conditions and the Bishop analytic exosphere model. *J. Geophys. Res.* 117, A03311. <http://dx.doi.org/10.1029/2011JA017074>.
- Picone, J.M., Hedin, A.E., Drob, D.P., Aikin, A.C., 2002. NRLMSISE-00 empirical model of the atmosphere: statistical comparisons and scientific issues. *J. Geophys. Res.* Space Phys. 107 (A12), 1468.
- Radicella, S.M., 2009. The NeQuick model genesis, uses and evolution. *Ann. Geophys.* 52 (3–4), 417–422.
- Richards, P.G., Torr, D.G., 1985. Seasonal, diurnal, and solar cyclical variations of the limiting H+ flux in the Earth's topside ionosphere. *J. Geophys. Res.* 90, 5261.
- Richards, P.G., 1986. Thermal electron quenching of N(2D): consequences for the ionospheric photoelectron flux and the thermal electron temperature. *Planet. Space Sci.* 34 (8), 689–694.
- Richards, P.G., 1991. An improved algorithm for determining neutral winds from the height of the F2 peak electron density. *J. Geophys. Res.* Space Phys. 96 (A10), 17839–17846.
- Richards, P.G., Buonsanto, M.J., Reinisch, B.W., Holt, J., Fennelly, J.A., Scali, J.L., Comfort, R.H., Germany, G.A., Spann, J., Brittnacher, M., Fok, M.-C., 2000. On the relative importance of convection and temperature on the behavior of the ionosphere in North America during January, 6–12, 1997. *J. Geophys. Res.* 105, 12763–12776.
- Richards, P.G., 2001. Seasonal and solar cycle variations of the ionospheric peak electron density: comparison of measurement and models. *J. Geophys. Res.* Space Phys. 106 (A7), 12803–12819.
- Richards, P.G., Woods, T.N., Peterson, W.K., 2006. HEUVAC: a new high resolution solar EUV proxy model. *Adv. Space Res.* 37 (2), 315–322.
- Richards, P.G., Nicolls, M.J., Heinselman, C.J., Sojka, J.J., Holt, J.M., Meier, R.R., 2009. Measured and modeled ionospheric densities, temperatures, and winds during the IPY. *J. Geophys. Res.* 114, A12317. <http://dx.doi.org/10.1029/2009JA014625>.
- Richards, P.G., Bilitza, D., Voglozin, D., 2010a. Ion density calculator (IDC): a new efficient model of ionospheric ion densities. *Radio Sci.* 45 (5), RS5007.
- Richards, P.G., Meier, R.R., Wilkinson, P.J., 2010b. On the compatibility of satellite measurements of thermospheric composition and solar EUV irradiance with ground-based ionospheric electron density data. *J. Geophys. Res.* 115, A10309. <http://dx.doi.org/10.1029/2010JA015368>.
- Richards, P.G., 2011. Reexamination of ionospheric photochemistry. *J. Geophys. Res.* 116, A08307. <http://dx.doi.org/10.1029/2011JA016613>.
- Richards, P.G., Nicolls, M.J., St.-Maurice, J.-P., Goodwin, L., Ruohoniemi, J.M., 2014. Investigation of sudden electron density depletions observed in the dusk sector by the Poker Flat, Alaska incoherent scatter radar in summer. *J. Geophys. Res.* Space Phys. 119. <http://dx.doi.org/10.1002/2014JA020541>.
- Schunk, R.W., Nagy, A.F., 1978. Electron temperatures in F-Region of ionosphere – theory and observations. *Rev. Geophys.* 16 (3), 355–399.
- Solomon, S.C., Woods, T.N., Didkovsky, L.V., Emmert, J.T., Qian, L., 2010. Anomalous low solar extremeultraviolet irradiance and thermospheric density during solar minimum. *Geophys. Res. Lett.* 37, L16103. <http://dx.doi.org/10.1029/2010GL044468>.
- Stankov, S.M., 2002. Empirical modelling of ion transition levels based on satellite in-situ measurements. *C. R. Acad. Bul. Sci.* 55 (1), 35–40.
- Stankov, S.M., Jakowski, N., Heise, S., Muhtarov, P., Kutiev, I., Warnant, R., 2003. A new method for reconstruction of the vertical electron density distribution in the upper ionosphere and plasmasphere. *J. Geophys. Res.* 108 (A5), 1164.
- Stankov, S.M., Stegen, K., Muhtarov, P., Warnant, R., 2011. Local ionospheric electron density profile reconstruction in real time from simultaneous ground-based GNSS and ionosonde measurements. *Adv. Space Res.* 47 (7), 1172–1180.
- Taylor, H.A., 1973. Parametric description of thermospheric ion composition results. *J. Geophys. Res.* 78 (1), 315–319.
- Titheridge, J.E., 1976. Ion transition heights from topside electron density profiles. *Planet. Space Sci.* 24 (3), 229–245.
- Torr, M.R., Torr, D.G., Richards, P.G., Yung, S.P., 1990. Mid- and low-latitude model of thermospheric emissions: 1. O+ (<sup>2</sup>P) 7320 Å and N2 (<sup>2</sup>P) 3371 Å. *J. Geophys. Res.* Space Phys. 95 (A12), 21147–21168.
- Trísková, L., Truhlík, V., Šmilauer, J., Shultchishin, Y.A., 1998. Comparison of O+H+ and O+(H+ + He+) transition levels. *Adv. Space Res.* 22 (6), 895–898.
- Trísková, L., Truhlík, V., Šmilauer, J., 2001. Empirical modeling of the upper transition height for low and middle latitudes. *Adv. Space Res.* 27 (1), 111–114.
- Trísková, L., Truhlík, V., Šmilauer, J., 2003. An empirical model of ion composition in the outer ionosphere. *Adv. Space Res.* 31 (3), 653–663.
- Truhlík, V., Trísková, L., Šmilauer, J., 2001. Improved electron temperature model and comparison with satellite data. *Adv. Space Res.* 27 (1), 101–109.
- Truhlík, V., Trísková, L., Šmilauer, J., 2005. Manifestation of solar activity in the global topside ion composition – a study based on satellite data. *Ann. Geophys.* 23 (7), 2511–2517.
- Woods, T.N., Chamberlin, P.C., Peterson, W.K., Meier, R.R., Richards, P.G., Strickland, D.J., Qian, G.L., Solomon, S.C., Iijima, B.A., Mannucci, A.J., Tsurutani, B.T., 2008. XUV photometer system (XPS): improved solar irradiance algorithm using Chianti spectral models. *Sol. Phys.* . <http://dx.doi.org/10.1007/s11207-008-9196-6>
- Zakharenkova, I.E., Krankowski, A., Bilitza, D., Cherniak, Iu.V., Shagimuratov, I.I., Sieradzki, R., 2011. Comparative study of foF2 measurements with IRI-2007 model predictions during extended solar minimum. *Adv. Space Res.* 51 (2013), 620–629. <http://dx.doi.org/10.1016/j.asr.2011.11.015>.